

RESEARCH ARTICLE

The Influence of Immunization Route, Tissue Microenvironment, and Cytokine Cell Milieu on HIV-Specific CD8⁺ T Cells Measured Using Fluidigm Dynamic Arrays

Shubhanshi Trivedi, Charani Ranasinghe*

Molecular Mucosal Vaccine Immunology Group, Department of Immunology, The John Curtin School of Medical Research, The Australian National University, Canberra ACT, Australia

* charani.ranasinghe@anu.edu.au



OPEN ACCESS

Citation: Trivedi S, Ranasinghe C (2015) The Influence of Immunization Route, Tissue Microenvironment, and Cytokine Cell Milieu on HIV-Specific CD8⁺ T Cells Measured Using Fluidigm Dynamic Arrays. PLoS ONE 10(5): e0126487. doi:10.1371/journal.pone.0126487

Academic Editor: R. Keith Reeves, Harvard Medical School, UNITED STATES

Received: December 16, 2014

Accepted: April 3, 2015

Published: May 6, 2015

Copyright: © 2015 Trivedi, Ranasinghe. This is an open access article distributed under the terms of the [Creative Commons Attribution License](https://creativecommons.org/licenses/by/4.0/), which permits unrestricted use, distribution, and reproduction in any medium, provided the original author and source are credited.

Data Availability Statement: All data are in the paper and its Supporting Information files.

Funding: This work was supported by NHMRC project grant 525431 (C.R.), development grant award APP1000703, Bill and Melinda Gates Foundation GCE Phase I grant OPP1015149 (C.R.) and ACH2 EOJ grants (C.R.). The funders had no role in study design, data collection and analysis, decision to publish, or preparation of the manuscript.

Competing Interests: The authors have declared that no competing interests exist.

Abstract

Thirty different genes including cytokines, chemokines, granzymes, perforin and specifically integrins were evaluated in Peyer's patch-KdGag_{197–205}-specific CD8⁺ T cells (pools of 100 cells) using Fluidigm 48.48 Dynamic arrays following three different prime-boost immunization strategies. Data revealed that the route of prime or the booster immunization differentially influenced the integrin expression profile on gut KdGag_{197–205}-specific CD8⁺ T cells. Specifically, elevated numbers of integrin αE and αD expressing gut KdGag_{197–205}-specific CD8⁺ T cells were detected following mucosal but not systemic priming. Also, αE/β7 and αD/β2 heterodimerization were more noticeable in an intranasal (i.n./i.n. vaccination setting compared to i.n./intramuscular (i.m) or i.m./i.m. vaccinations. Moreover, in all vaccine groups tested α4 appeared to heterodimerize more closely with β7 then β1. Also MIP-1β, RANTES, CCR5, perforin and integrin α4 bio-markers were significantly elevated in i.n./i.m. and i.m./i.m. immunization groups compared to purely mucosal i.n./i.n. delivery. Furthermore, when wild type (WT) BALB/c and IL-13 knock-out (KO) mice were immunized using i.n./i.m. strategy, MIP-1α, MIP-1β, RANTES, integrins α4, β1 and β7 mRNA expression levels were found to be significantly different, in mucosal verses systemic KdGag_{197–205}-specific CD8⁺ T cells. Interestingly, the numbers of gut KdGag_{197–205}-specific CD8⁺ T cells expressing gut-homing markers α4β7 and CCR9 protein were also significantly elevated in IL-13 KO compared to WT control. Collectively, our findings further corroborate that the route of vaccine delivery, tissue microenvironment and IL-13 depleted cytokine milieu can significantly alter the antigen-specific CD8⁺ T cell gene expression profiles and in turn modulate their functional avidities as well as homing capabilities.

Introduction

It is now well established that route of vaccine delivery can greatly influence the quality of HIV-specific CD8⁺ T cell immunity. Purely systemic immunization strategies intramuscular

(i.m.) or intravenous (i.v.) immunizations) generate mainly long-lasting systemic immunity, whereas mucosal immunization (i.n., intrarectal (i.r.) or oral) is able to induce “long lasting” mucosal immune responses at the local and distant mucosa [1–4]. It has been shown that macaques vaccinated with i.m. DNA-HIV vaccine priming followed by i.n. or i.r. fowlpox virus (FPV)-HIV booster immunization generated enhanced local T-cell immunity in cervico-vaginal tissues, and they were protected against a mucosal SHIV challenge [5]. Studies where i.m. pDNA-HIV/ i.n. FPV-HIV; i.n. FPV-HIV/ i.m. attenuated vaccinia virus (VV)-HIV and i.n. VV-HIV/ i.m. FPV-HIV were evaluated, i.n. FPV-HIV prime followed by i.m. VV-HIV booster vaccination has shown to induce robust polyfunctional HIV-specific T cell immunity compared to the two other prime-boost vaccination strategies [6]. Notably, control of HIV replication in elite controllers (< 1%) have been associated with enhanced high avidity polyfunctional HIV-specific CD8⁺ T cells [7, 8]. Our studies also clearly demonstrated that rFPV was an excellent mucosal delivery vector. We have also shown that compared to purely systemic (i.m. FPV-HIV/ i.m. VV-HIV) immunization regime, i.n. FPV-HIV prime followed by i.m. VV-HIV booster immunization strategy induce robust long lasting CD8⁺ systemic and mucosal T cell responses to HIV-1 vaccine antigens [9], which were also of higher avidity [10, 11]. Furthermore, purely mucosal immunization i.n./i.n. or combined mucosal systemic i.n./i.m. immunization induced HIV-specific CD8⁺ T cells with lower IL-4 and IL-13 expression compared to systemic immunization (i.m./i.m.), which were of higher avidity. Later studies using IL-13 KO mice have confirmed that IL-13 can significantly dampen the induction of effector and memory CD8⁺ T cells of higher avidity following vaccination [10, 12].

Studies have also shown that tissue microenvironment (*i.e.* mucosal vs. systemic compartments) influence the nature of immune responses induced at mucosal and systemic sites [13–15]. Unlike systemic compartment, due to the ability of antigens to be processed and presented via the microfold or M cells, immune responses induced in the mucosal compartment is uniquely different [16, 17]. It is known that, locally activated mucosal DCs but not splenic-DCs have the ability to imprint T cells with mucosal homing markers [18, 19]. For example, DCs purified from Peyer’s patches and mesenteric lymph nodes (MLNs) but not from spleen or peripheral lymph nodes induce T cell expression of both $\alpha_4\beta_7$ and CCR9 *in vitro* and licence effector/memory T cells to home preferentially to intestinal epithelium [18, 19]. Notably, only gut-DCs (but not DCs from other lymphoid organs) can produce retinoic acid from retinol (vitamin A), and it has been shown that retinoic acid plays a critical role in imprinting of gut-homing specificities on T cells [20]. These studies highlights the importance of mucosal vaccination in the process of inducing long-lived mucosal-specific T cell immunity. Unfortunately, no clear biomarkers are currently available to measure HIV-specific mucosal vaccine-specific CD8⁺ T cell immunity, during human or NHP HIV vaccine trials, obtaining enough HIV-specific CD8 T cells from gut or rectal biopsies to evaluate mucosal immunity can be a difficult task. Specifically, due to small sample size obtaining meaningful data from FACS ELISPOT, can be a difficult task [21]. Thus, finding new biomarkers that can be used to evaluate mucosal immunity, under these circumstances can be of great importance, and this forms the basis of this project.

Therefore, in this study, with the hope of identifying gene expression profiles unique to mucosal and systemic vaccination, thirty genes comprised of cytokines, chemokines, granzymes, perforin, markers which are involved in immune regulation and integrins (Table 1), were evaluated using Fluidigm 48.48 Dynamic array system. Specifically the array of integrins were selected as i) some of these molecules have shown to provoke lymphocyte homing to specific tissues, and ii) enhanced expression of certain homing receptors on antigen-specific T cells following mucosal vaccination has been associated with mucosal T cell homing and control of viral replication at the mucosae [22–24]. In this study mRNA expression profiles were evaluated in pools of hundred gut K^dGag_{197–205}-specific (tetramer-specific) CD8⁺ T cells obtained

Table 1. Genes of interest used in this study for mRNA quantification using Fluidigm 48.48 dynamic array nanofluidic chip.

N	Gene symbol	Gene name	Category	Reference sequence	Assay ID
1	RpL32	Ribosomal protein L32	Endogenous standards	NM_172086.2	Mm02528467_g1
2	IFN- γ	Interferon gamma	Cytokines	NM_008337.3	Mm01168134_m1*
3	IL-2	Interleukin 2	Cytokines	NM_008366.2	Mm00434256_m1*
4	TNF- α	Tumor necrosis factor alpha	Cytokines	NM_013693.2	Mm00443258_m1*
5	IL-4	Interleukin-4	Cytokines	NM_021283.2	Mm00445259_m1*
6	IL-13	Interleukin-13	Cytokines	NM_008355.3	Mm00434204_m1*
7	IL-17	Interleukin-17	Cytokines	NM_010552.3	Mm00439618_m1*
8	MIP-1 α (CCL3)	chemokine (C-C motif) ligand 3	Chemokines	NM_011337.2	Mm00441258_m1*
9	MIP-1 β (CCL4)	chemokine (C-C motif) ligand 4	Chemokines	NM_013652.2	Mm00443111_m1*
10	RANTES (CCL5)	chemokine (C-C motif) ligand 5	Chemokines	NM_013653.3	Mm01302428_m1*
11	Gzm A	Granzyme A	Protease	NM_010370.2	Mm00439191_m1*
12	Gzm B	Granzyme B	Protease	NM_013542.2	Mm00442834_m1*
13	Gzm C	Granzyme C	Protease	NM_010371.2	Mm01313651_m1*
14	Prf1	Perforin 1	Defense protein	NM_011073.3	Mm00812512_m1*
15	Sell (CD62L)	L-selectin	Cell adhesion molecule	NM_011346.1	Mm00441291_m1*
16	Selp1g (Psgl1)	P-selectin ligand	Receptor	NM_009151.3	Mm01204601_m1*
17	CD69	CD69 antigen	Receptor	NM_001033122.3	Mm01183378_m1*
18	CCR5	Chemokine (C-C motif) receptor 5	Receptor	NM_009917.5	Mm01216171_m1*
19	CCR7	Chemokine (C-C motif) receptor 7	Receptor	NM_007719.2	Mm01301785_m1*
20	CCR9	Chemokine (C-C motif) receptor 9	Receptor	NM_009913.5	Mm02620030_s1*
21	CCR10	Chemokine (C-C motif) receptor 10	Receptor	NM_007721.4	Mm01292449_m1*
22	Itga4	Integrin alpha 4	Integrin	NM_010576.3	Mm00439770_m1*
23	ItgaE	Integrin alpha E	Integrin	2 Refseqs	Mm00434443_m1*
24	ItgaL	Integrin alpha L	Integrin	4 Refseqs	Mm00801807_m1*
25	ItgaM (CD11b)	Integrin alpha M	Integrin	2 Refseqs	Mm00434455_m1*
26	ItgaX (CD11c)	Integrin alpha X	Integrin	NM_021334.2	Mm00498698_m1*
27	ItgaD (CD11d)	Integrin alpha D	Integrin	NM_001029872.2	Mm01159115_m1*
28	Itgb1	Integrin beta 1 (fibronectin receptor beta)	Integrin	NM_010578.2	Mm01253228_g1*
29	Itgb2	Integrin beta 2	Integrin	NM_008404.4	Mm00434513_m1*
30	Itgb7	Integrin beta 7	Integrin	NM_013566.2	Mm00442916_m1*

Note: In assay ID column * indicates the relevant accession numbers of the TaqMan primer probe sets used in the study obtained from Applied Biosystems (Life Technologies, USA).

doi:10.1371/journal.pone.0126487.t001

from i.n./i.n. (purely mucosal), i.n./i.m. (mucosal/systemic) and i.m./i.m. (purely systemic) FPV-HIV/VV-HIV prime-boost vaccinated BALB/c mice and hundred gut and splenic K^dGag_{197–205}-specific CD8⁺ T cells obtained from BALB/c and IL-13 KO animals following i.n./i.m. immunization. In our previous studies mucosal immunization [10], and IL-13 depleted cell milieu has shown to promote the induction of higher avidity HIV-specific CD8⁺ T cells, where avidity profile of IL-13 KO > WT BALB/C mice [12].

Results

Mucosal and systemic vaccination can induce distinct mRNA expression profiles in gut-K^dGag_{197–205}-specific CD8⁺ T cells

WT BALB/c (n = 4–5) were primed with FPV-HIV and boosted with VV-HIV vaccine using i.n./i.n., i.n./i.m. or i.m./i.m. vaccine regimes as indicated in methods, fourteen days post booster

immunization gut K^dGag_{197–205}-specific CD8⁺ T cell were sorted in groups of hundred cells and mRNA expression profiles of 30 genes of interest (Table 1) were evaluated using Fluidigm 48.48 Dynamic arrays. When expression of cytokines IFN- γ , TNF- α , IL-2, IL-4, IL-13 and IL-17 mRNA by gut K^dGag_{197–205}-specific CD8⁺ T cells were evaluated, although no IFN- γ , IL-2, IL-4, IL-13 and IL-17 mRNA were detected, majority of the pools of hundred gut K^dGag_{197–205}-specific CD8⁺ T cells obtained from the three immunization regimes (i.n./i.n.- 9 out of 9; i.n./i.m. and i.m./i.m.- 8 out of 10, i.e. 80–100%) expressed TNF- α , and the expression profile between the three regimes were very similar (Fig 1a).

When chemokines MIP-1 α , MIP-1 β and RANTES mRNA expression profiles were evaluated, data indicated that although the level of MIP-1 α mRNA expression was similar between the three regimes, the number of hundred gut K^dGag_{197–205}-specific CD8⁺ T pools expressing MIP-1 α were higher in the i.n./i.m. and i.m./i.m. regimes compared to the purely mucosal i.n./i.n. prime-booster regime (Fig 1b). Data also revealed that all cell pools (i.n./i.n.- 9/9, i.n./i.m. and i.m./i.m.-10/10) expressed MIP-1 β and RANTES mRNA and the expression level of MIP-1 β mRNA was significantly higher in the i.n./i.m. and i.m./i.m. groups and the RANTES mRNA in the i.m./i.m. group compared to the i.n./i.n. group (MIP-1 β i.n./i.n. vs. i.n./i.m. $p = 0.045$ and

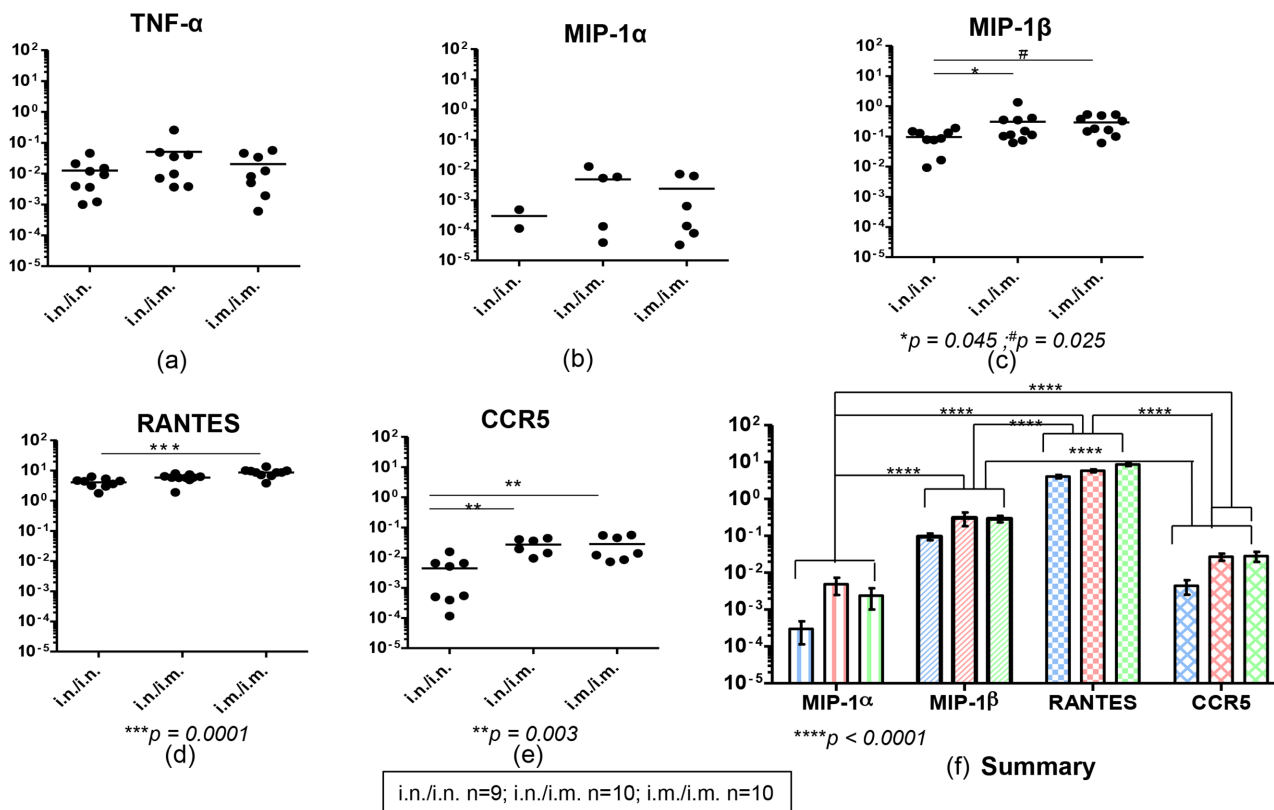


Fig 1. Evaluation of TNF- α , chemokines and chemokine receptor mRNA expression in gut K^dGag_{197–205}-specific CD8⁺ T cells following i.n./i.n., i.n./i.m. and i.m./i.m. vaccination. BALB/c mice (n = 4–5 per group) were primed i.n. or i.m. with FPV-HIV and boosted i.n. or i.m. with VV-HIV, fourteen days post boost immunization Peyer's patches were pooled from all animals and cells were then stained with K^dGag_{197–205} tetramer. These gut K^dGag_{197–205}-specific CD8⁺ T cells were sorted in hundred cell pools (i.n./i.n. n = 9, i.n./i.m. n = 10 and i.m./i.m. n = 10 hundred cell pools) in a 96-wells plate, cDNA was synthesized and mRNA expression profiles were evaluated using Fluidigm 48.48 dynamic arrays as described in methods. The log mRNA expression normalised to housekeeping gene L32 ($2^{-\Delta\text{CT}}$, where $\Delta\text{CT} = \text{CT}_{\text{gene}} - \text{CT}_{\text{L32}}$) of TNF- α (a), MIP-1 α (b), MIP-1 β (c), RANTES (d), CCR5 (e) is shown. All chemokines tested and CCR5 expression in gut K^dGag_{197–205}-specific CD8⁺ T cells following i.n./i.n. (blue), i.n./i.m. (red) and i.m./i.m. (green) vaccination is summarized (f). In each plot (a-e), black circles indicate a pool of hundred gut K^dGag_{197–205}-specific CD8⁺ T cells and black line indicate mean expression. The experiment was repeated three times. Data represent the three experiments.

doi:10.1371/journal.pone.0126487.g001

i.n./i.n. vs. i.m./i.m. $p = 0.025$; RANTES i.n./i.n. vs i.m./i.m. $p = 0.0001$) (Fig 1c and 1d). The level of CCR5 mRNA expression by these gut K^dGag_{197–205}-specific CD8⁺ cells were also found to be similar to that of MIP-1 β where i.n./i.n. vs. i.n./i.m. and i.n./i.n. vs i.m./i.m. were significantly elevated $p = 0.003$ (Fig 1e). In all three immunization regimes tested, the hierarchy of these chemokine and/or their receptor mRNA expression by gut-K^dGag_{197–205}-specific CD8⁺ T cells was found to be RANTES > MIP-1 β > CCR5 > MIP-1 α (Fig 1f).

When the levels of granzymes (A,B and C) and perforin mRNA expression by gut-K^dGag_{197–205}-specific CD8⁺ T cells were compared, in all three immunization regimes major proportion of the hundred cell pools were found to express granzyme A and B mRNAs (60–90%) but no granzyme C expression was detected in any of the immunization regimes tested. Also, the levels of granzyme A and B mRNA expression were found to be similar between the three immunization regimes tested (Fig 2a and 2b). In contrast, the number of perforin expressing gut-K^dGag_{197–205}-specific CD8⁺ T cell pools were lower (40–60%), and the level of perforin expression was significantly higher in the i.n./i.m. and i.m./i.m. regimes compared to i.n./i.n. strategy (i.n./i.n. vs. i.n./i.m. $p = 0.035$ and i.n./i.n. vs. i.m./i.m. $p = 0.043$) (Fig 2c).

Furthermore, when the expression of CD62L (also represented as ‘sell’), CD69, CCR7, CCR9, CCR10 and P-selectin ligand (selplg) mRNA by gut-K^dGag_{197–205}-specific CD8⁺ T cells were evaluated between the three immunization regimes, no expression of CD62L, CCR9 and CCR10 were detected. However, compared to CCR7, lower numbers of gut-K^dGag_{197–205}-specific CD8⁺ T cell pools were found to be positive for P-selectin ligand and CD69 and no significant differences in

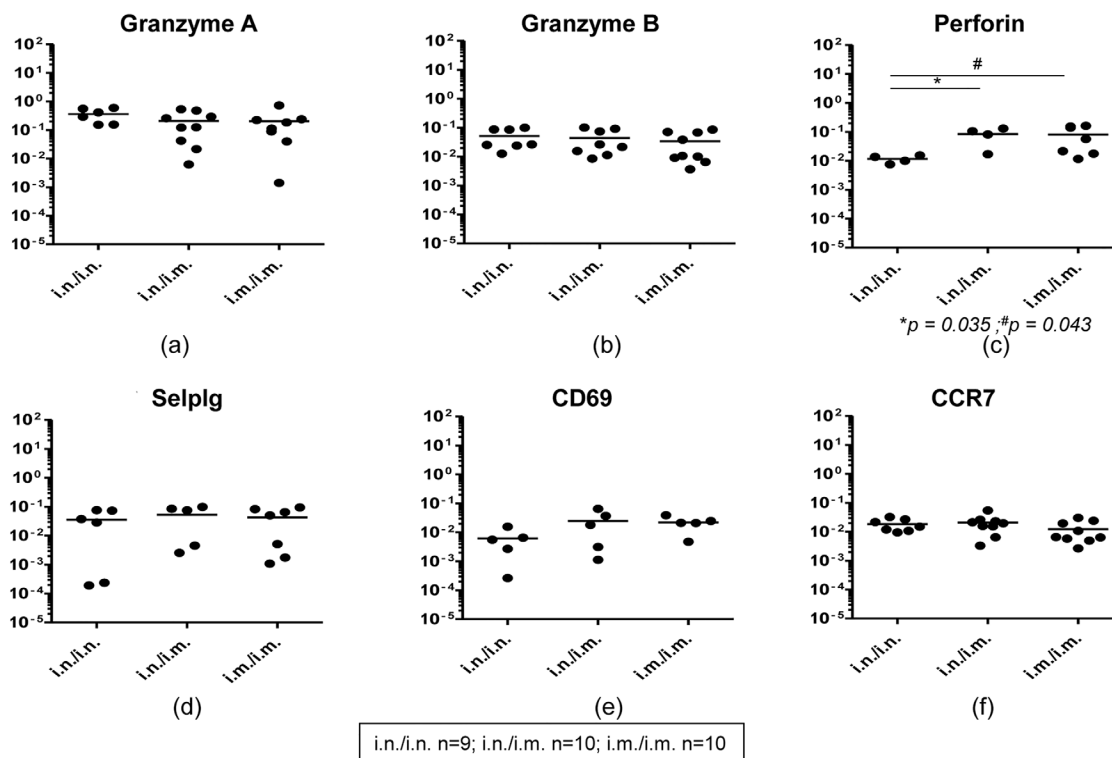


Fig 2. Evaluation of granzymes, perforin and receptor mRNA expression in gut K^dGag_{197–205}-specific CD8⁺ T cells following i.n./i.n., i.n./i.m. and i.m./i.m. vaccination. mRNA expression profile in i.n./i.n., i.n./i.m. and i.m./i.m. immunized pools of hundred gut K^dGag_{197–205}-specific CD8⁺ T cells (i.n./i.n. n = 9, i.n./i.m. n = 10 and i.m./i.m. n = 10 pools) were evaluated using Fluidigm 48.48 dynamic arrays as described in methods. The log mRNA expression normalised to housekeeping gene L32 ($2^{-\Delta CT}$) of granzyme-A (a), granzyme-B (b), perforin (c), selplg or P-selectin ligand (d), CD69 (e) and CCR9 (f) is shown. In each plot (a-f), black circles indicate a pool of hundred gut K^dGag_{197–205}-specific CD8⁺ T cells and black line indicate mean expression. The experiment was repeated three times. Data represent the three experiments.

doi:10.1371/journal.pone.0126487.g002

the expression levels of these mRNA were detected between three immunization regimes tested (Fig 2d–2f).

Different routes of vaccine delivery can induce distinct integrin mRNA expression profiles in gut- K^dGag_{197–205}-specific CD8⁺ T cells

It is established that $\alpha 4$ can heterodimerize with either $\beta 7$ or $\beta 1$ while αE can only heterodimerize with $\beta 7$. In the three immunization regimes tested, all the pools of hundred gut-K^dGag_{197–205}-specific CD8⁺ T cells (100%) were found to express integrin $\alpha 4$, and the expression was significantly higher in i.n./i.m. and i.m./i.m. compared to the purely mucosal i.n./i.n. immunization regime (i.n./i.n. vs. i.n./i.m. and i.n./i.n. vs. i.m./i.m. $p = 0.003$) (Fig 3a). Data revealed that 100% of gut-K^dGag_{197–205}-specific CD8⁺ T cells were also positive for integrins $\beta 1$ and $\beta 7$ mRNA in all the groups tested (Fig 3b & 3e). The expression level hierarchy of $\beta 1$ mRNA was i.n./i.m. > i.m./i.m. > i.n./i.n. whereas expression level of $\beta 7$ mRNA was similar in all the groups (Fig 3b & 3e). Interestingly, when the $\alpha 4$, $\beta 1$ and $\beta 7$ mRNA expression by gut-K^dGag_{197–205}-specific CD8⁺ T cells were compared between the three immunization regimes (Fig 3c), $\alpha 4$ and $\beta 7$ expression profiles were found to be relatively higher and closely linked specifically in i.n./i.n. and i.n./i.m. groups compared to the mean expression level of $\alpha 4$ and $\beta 1$ mRNAs in all the groups (Fig 3c).

Although the levels of integrin αE (which can also pair with $\beta 7$ integrin) mRNA expression were similar between the three immunization regimes, 90–100% (i.n./i.n.- 9/9, i.n./i.m.- 9/10) of the pools of hundred gut-K^dGag_{197–205}-specific CD8⁺ T cell obtained from i.n./i.n. and i.n./i.m.

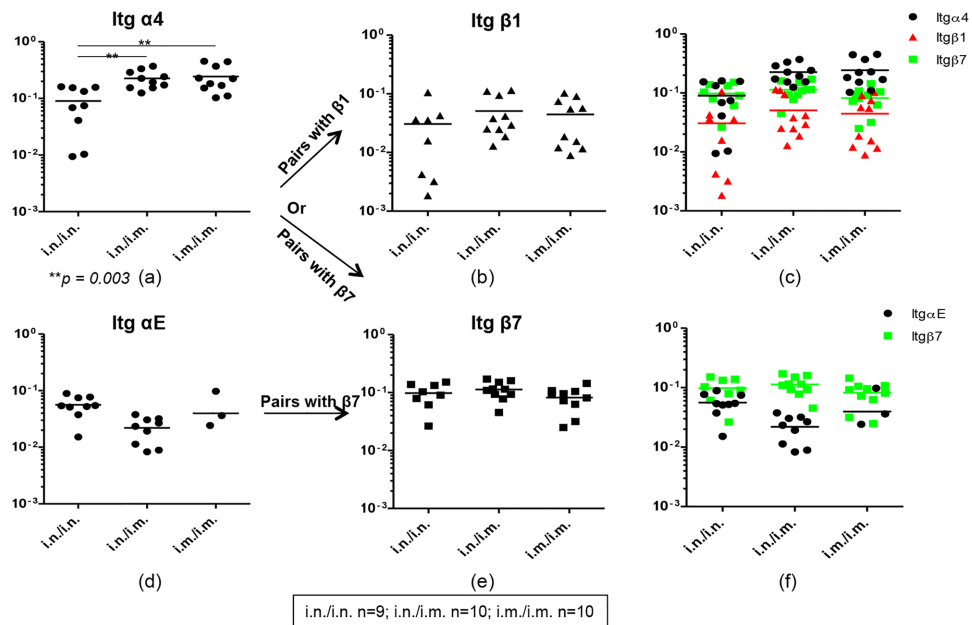


Fig 3. Evaluation of integrins $\alpha 4$, αE , $\beta 1$ and $\beta 7$ mRNA expression in gut K^dGag_{197–205}-specific CD8⁺ T cells following i.n./i.n., i.n./i.m. and i.m./i.m. vaccination. Integrins mRNA expression profile in i.n./i.n., i.n./i.m. and i.m./i.m. immunized pools of hundred gut K^dGag_{197–205}-specific CD8⁺ T cells (i.n./i.n. n = 9, i.n./i.m. n = 10 and i.m./i.m. n = 10 pools) were evaluated using Fluidigm 48.48 dynamic arrays as described in methods. The log mRNA expression normalised to housekeeping gene L32 of integrin $\alpha 4$ (a), $\beta 1$ (b), $\alpha 4$ (black circle) which can pair up with $\beta 1$ (red triangle) and $\beta 7$ (green square) (c), αE (d), $\beta 7$ (e) and αE (black circle) which can pair up with $\beta 7$ (green square) (f) is shown. The p values were calculated using one-way ANOVA. In all the plots circles or triangles or square indicate a pool of hundred gut K^dGag_{197–205}-specific CD8⁺ T cells and line indicate mean expression. The experiment was repeated three times. Data represent the three experiments.

doi:10.1371/journal.pone.0126487.g003

regimes (mucosally prime groups) expressed integrin αE compared to the purely systemic immunization strategy (only 3/10 or 30% of hundred cell pools expressed αE) (Fig 3d). Next when the αE and $\beta 7$ mRNA expression by gut- K^d Gag_{197–205}-specific CD8⁺ T cells were compared between the three immunization regimes, αE and $\beta 7$ expression profiles were found to be more closely associated in the i.n./i.n. purely mucosal vaccinated group compared to the i.n./i.m combined mucosal systemic or i.m./i.m. purely systemic vaccinated groups (Fig 3f).

Furthermore, integrins αL , αM , αX and αD which can heterodimerize with $\beta 2$ integrin were evaluated in the three immunization regimes. Very low proportion of cell pools (1/10) were found to express integrin αL in i.n./i.m. group compared to the purely mucosal and purely systemic immunization groups, also the expression levels were not significantly different between the three groups tested (Fig 4a). Data indicated that higher numbers of hundred cell pools expressed integrin αM mRNA in i.n./i.m. group (~50%) and i.m./i.m. group (~30%) compared to i.n./i.n. group (~10%) (Fig 4b). Also, the expression was significantly higher in i.n./i.m and i.m./i.m. compared to purely mucosal i.n./i.n. regime (Fig 4b). Major proportion of the hundred cell pools (60%) obtained from i.n./i.m. group were found to express integrin αX , and the expression levels were also found to be relatively higher in this group compared to purely mucosal and purely systemic immunization regimes (Fig 4c). Unlike the expression pattern of integrins αM and αX positive gut- K^d Gag_{197–205}-specific CD8⁺ T cells where the expression profile hierarchy was i.n./i.m. > i.m./i.m. > i.n./i.n., higher proportions (80%) of gut- K^d Gag_{197–205}-specific CD8⁺ T cells expressed integrin αD mRNA in purely mucosal i.n./i.n. regime compared to i.n./i.m. (10%) and i.m./i.m. (20%) groups (Fig 4d). Interestingly, in all the immunization regimes tested, 90–100% of gut- K^d Gag_{197–205}-specific CD8⁺ T cells were found to express integrin $\beta 2$ and also the expression levels were similar between the groups (Fig 4e). Next the integrin αD and $\beta 2$ mRNA expression by gut- K^d Gag_{197–205}-specific CD8⁺ T cells were compared between the three immunization regimes (Fig 4f). Based on 80% of cells in the i.n./i.n. group expressing integrin αD and 100% of cells also expressing integrin $\beta 2$, data suggest that integrin αD and $\beta 2$ could be

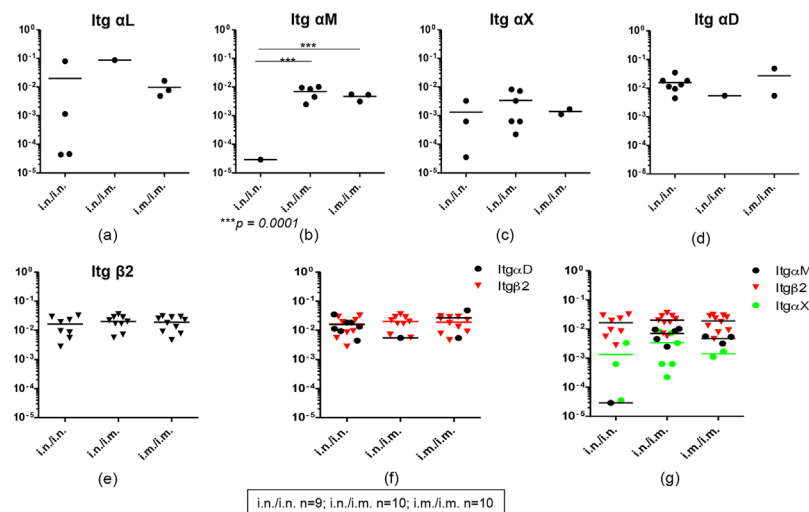


Fig 4. Evaluation of integrins αL , αM , αX , αD and $\beta 2$ mRNA expression in gut K^d Gag_{197–205}-specific CD8⁺ T cells following i.n./i.n., i.n./i.m. and i.m./i.m. vaccination. The log mRNA expression normalised to housekeeping gene L32 of integrin αL (a), αM (b), αX (c), αD (d), $\beta 2$ (e) αD (black circle) and $\beta 2$ (inverted red triangle) (f) and αX (green circle), αM (black circle) which can pair up with $\beta 2$ (inverted red triangle) (g) is shown. The p values were calculated using one-way ANOVA. In all the plots circles or triangles or square indicate a pool of hundred gut K^d Gag_{197–205}-specific CD8⁺ T cells and line indicate mean expression. The experiment was repeated three times. Data represent the three experiments.

doi:10.1371/journal.pone.0126487.g004

more closely associated with i.n. delivery compared to i.m. delivery (Fig 4f). Similarly, when integrin αM , αX and $\beta 2$ were compared between the three groups (Fig 4g), in i.n./i.m. and i.m./i.m. groups the integrins αM and $\beta 2$ were found to be relatively higher and closely associated compared to integrins αX and $\beta 2$ (Fig 4g).

WT BALB/c and IL-13 KO mice have distinct mRNA expression profiles in systemic and mucosal K^dGag_{197–205}-specific CD8⁺ T cells

We have shown that i.n. FPV-HIV/ i.m. VV-HIV immunization strategy can induce robust and sustained high avidity systemic and mucosal CD8⁺ T cell responses [10]. Thus, in this part of the study, WT BALB/c and IL-13 KO mice (n = 4–5) were immunized i.n. FPV-HIV/ i.m. VV-HIV strategy, 14 days post booster vaccination, gut and splenic K^dGag_{197–205}-specific CD8⁺ T cell were sorted in groups of hundred cells, and mRNA expression profiles of the above same 30 genes were evaluated using Fluidigm 48.48 Dynamic arrays (Table 1). Interestingly, no IL-2, IL-4, IL-13, IL-17 mRNA expression were detected in gut and splenic K^dGag_{197–205}-specific CD8⁺ T cells in all mice groups tested. IFN- γ were detected in 40–50% of the hundred cell pools obtained from spleen (WT BALB/c - 3/6, IL-13 KO - 2/5) and Peyer’s patch (WT BALB/c - 2/6, IL-13 KO - 4/9) and the IFN- γ mRNA expression level was relatively higher in splenic K^dGag_{197–205}-specific CD8⁺ T cells (WT spleen vs. Peyer’s patch *p* = 0.019) compared to Peyer’s patches (Fig 5a). Unlike IFN- γ mRNA expression, much greater proportion of cells were found to express TNF- α (WT BALB/c spleen - 6/6, Peyer’s patch - 5/6; and IL-13 KO spleen - 5/5, Peyer’s patch - 7/9), but no difference in the expression profiles were detected between gut and splenic K^dGag_{197–205}-specific CD8⁺ T cells obtained from the two mice groups (Fig 5b).

When chemokines MIP-1 α , MIP-1 β and RANTES mRNA expression in WT and IL-13 KO gut and splenic K^dGag_{197–205}-specific CD8⁺ T cells were evaluated, compared to MIP-1 β and RANTES relatively lower numbers of gut and splenic-K^dGag_{197–205}-specific CD8⁺ T cell pools expressed MIP-1 α mRNA (WT BALB/c spleen - 5/6, Peyer’s patch - 4/6; and IL-13 KO spleen - 4/5, Peyer’s patch - 5/9) (Fig 6a). In both WT and IL-13 KO groups, the expression levels of MIP-1 α

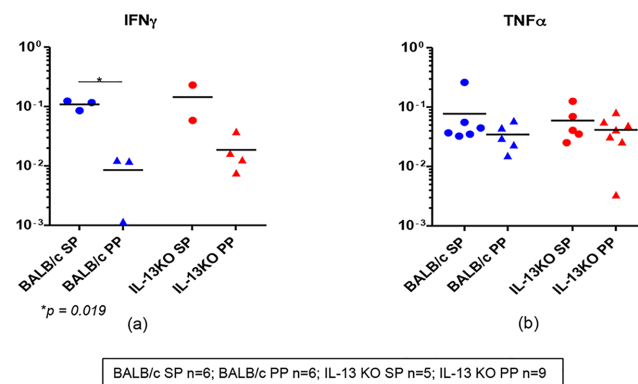


Fig 5. Evaluation of cytokine mRNA expression in WT BALB/c and IL-13 KO gut and splenic K^dGag_{197–205}-specific CD8⁺ T cells following i.n./i.m. vaccination. WT BALB/c and IL-13 KO mice (n = 4–5/ group) were prime-boost immunized with i.n. FPV-HIV/ i.m. VV-HIV. Fourteen days post booster vaccination mRNA expression profiles in gut and splenic K^dGag_{197–205}-specific CD8⁺ T cells were evaluated using Fluidigm 48.48 dynamic arrays as described in methods. WT BALB/c spleen (SP) and Peyer’s patch (PP) n = 6 pools of hundred K^dGag_{197–205}-specific CD8⁺ T cells are indicated by blue circle and triangle respectively. IL-13 KO mice spleen n = 5 and Peyer’s patch n = 9 pools of hundred K^dGag_{197–205}-specific CD8⁺ T cells are indicated by red circles and triangles respectively. Data indicate log mRNA expression of IFN- γ (a) and TNF- α (b) normalised to housekeeping gene L32. The experiment was repeated three times. Data represent the three experiments.

doi:10.1371/journal.pone.0126487.g005

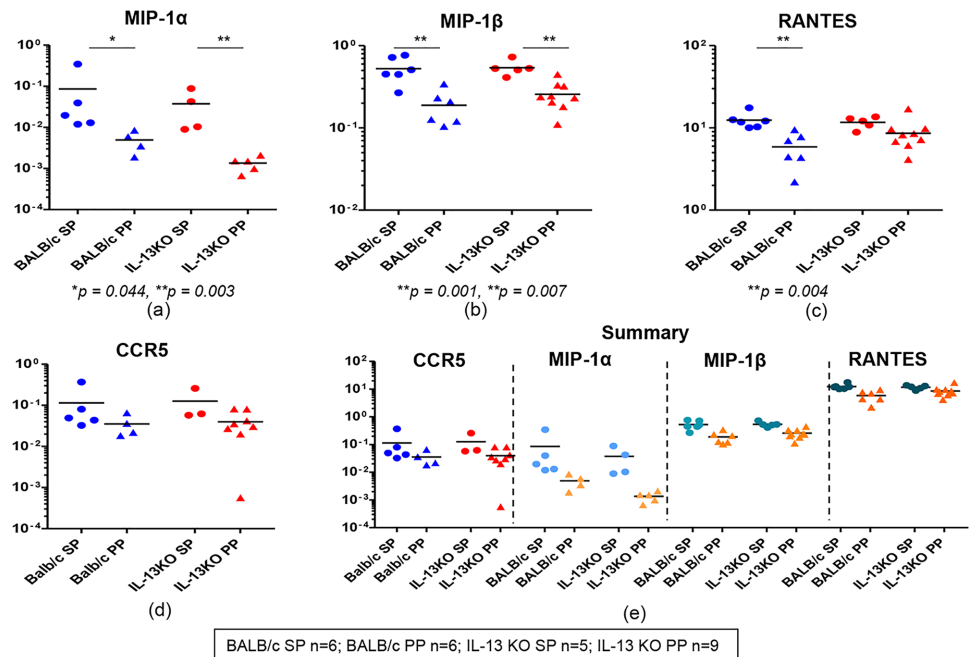


Fig 6. Evaluation of chemokines and chemokine receptor mRNA expression in WT BALB/c and IL-13 KO gut and splenic K^dGag_{197–205}-specific CD8⁺ T cells following i.n./i.m. vaccination. Exactly as in Fig 5 WT BALB/c and IL-13 KO mice (n = 4–5/ group) were prime-boost immunized with i.n. FPV-HIV/ i.m. VV-HIV. and mRNA expression profiles in gut and splenic K^dGag_{197–205}-specific CD8⁺ T cells were evaluated. WT BALB/c spleen (SP) and Peyer’s patch (PP) n = 6 pools of hundred K^dGag_{197–205}-specific CD8⁺ T cells are indicated by blue circle and triangle respectively. IL-13 KO mice spleen n = 5 and Peyer’s patch n = 9 pools of hundred K^dGag_{197–205}-specific CD8⁺ T cells are indicated by red circles and triangles respectively. Data indicate log mRNA expression of MIP-1α (a) MIP-1β (b) and RANTES (c) CCR5 (d) normalised to housekeeping gene L32. Fig 6e indicates the summary of chemokine and CCR5 data.

doi:10.1371/journal.pone.0126487.g006

were significantly elevated in splenic K^dGag_{197–205}-specific CD8⁺ T cells compared to Peyer’s patches (spleen vs. Peyer’s patch $p = 0.044$ and 0.003 respectively) (Fig 6a). Similarly, in all the groups tested even though 100% of K^dGag_{197–205}-specific CD8⁺ T cells were positive for MIP-1β and RANTES, the expression levels were significantly higher in spleen compared to Peyer’s patch (MIP-1β expression in WT and IL-13KO, spleen vs. Peyer’s patch $p = 0.001$ and 0.007 respectively; RANTES in WT group spleen vs. Peyer’s patch $p = 0.004$) (Fig 6b & 6c). Interestingly, in these groups the level of CCR5 mRNA expression between gut and splenic K^dGag_{197–205}-specific CD8⁺ T cells were very similar, and compared to RANTES and MIP-1β, the proportion of cells expressing CCR5 were relatively lower (WT BALB/c spleen - 5/6, Peyer’s patch - 4/6; and IL-13 KO spleen - 3/5, Peyer’s patch - 8/9) (Fig 6d). In WT BALB/c or IL-13 KO group the hierarchy of chemokine and/or their receptor mRNA expression by gut and splenic K^dGag_{197–205}-specific CD8⁺ T cells was found to be RANTES > MIP-1β > MIP-1α ≥ CCR5 (Fig 6e).

When the expression of granzyme A, B and C mRNA in WT and IL-13 KO gut and splenic K^dGag_{197–205}-specific CD8⁺ T cells were evaluated, major proportion of the hundred cell pools were found to express granzyme A and B mRNAs (80–100%) (Fig 7a & 7b) but no granzyme C expression was detected in any of the groups tested. Although the expression levels of granzyme A and B were found to be similar in WT and IL-13 KO splenic and gut K^dGag_{197–205}-specific CD8⁺ T cells (Fig 7a & 7b) 100% (9/9) of the IL-13 KO gut-specific cell pools expressed B. Interestingly, in both compartments in WT and IL-13 KO groups 80–100% of hundred cell pools were positive for perforin, but expression levels were relatively higher in spleen compared

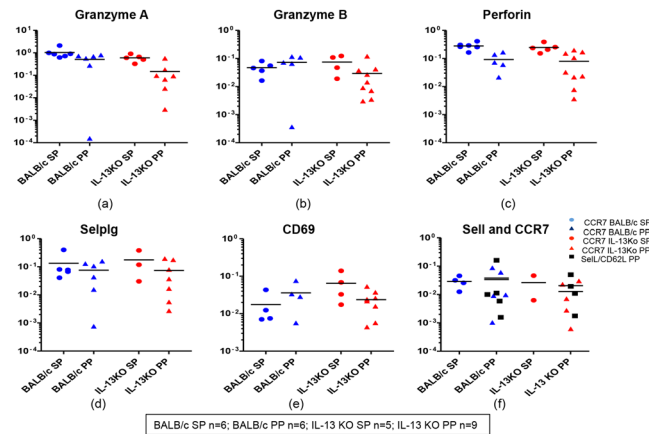


Fig 7. Evaluation of granzymes, perforin and receptor mRNA expression in WT BALB/c and IL-13 KO gut and splenic K^dGag_{197–205}-specific CD8⁺ T cells following i.n./i.m. vaccination. mRNA expression profiles in WT BALB/c and IL-13KO gut and splenic K^dGag_{197–205}-specific CD8⁺ T cells were evaluated using Fluidigm 48.48 dynamic arrays as described in methods. WT BALB/c spleen (SP) and Peyer’s patch (PP) n = 6 pools of hundred K^dGag_{197–205}-specific CD8⁺ T cells are indicated by blue circle and triangle respectively. IL-13 KO mice spleen n = 5 and Peyer’s patch n = 9 pools of hundred K^dGag_{197–205}-specific CD8⁺ T cells are indicated by red circles and triangles respectively. Data indicate log mRNA expression of granzyme A (a) granzyme B (b) perforin (c) selplg or P-selectin ligand (d) CD69 (e) and memory markers sell (CD62L) and CCR7 (f) normalised to housekeeping gene L32. The experiment was repeated three times. Data represent the three experiments.

doi:10.1371/journal.pone.0126487.g007

to Peyer’s patch (Fig 7c). Furthermore, in WT and IL-13 KO groups, similar proportions of cells were found to express P-selectin ligand and CD69 mRNA in both compartments (WT BALB/c spleen- 4 to 5/6, Peyer’s patch- 4 to 6/6; and IL-13 KO spleen- 3 to 4/5, Peyer’s patch- 7 to 8/9), and their expression levels were also very similar (Fig 7d & 7e).

Interestingly, when the memory markers CD62L and CCR7 mRNA expression was evaluated in all the groups, the CD62L mRNA expression was only detected in gut K^dGag_{197–205}-specific CD8⁺ (WT BALB/c 5/6 and IL-13 KO 4/9) whereas CCR7 mRNA expression was detected in both splenic and gut K^dGag_{197–205}-specific CD8⁺ T cells (WT BALB/c spleen- 4/6, Peyer’s patch- 5/6; and IL-13 KO spleen- 2/5, Peyer’s patch- 5/9) (Fig 7f). The expression levels of CCR7 mRNA were found to be similar in the two compartments (Fig 7f). However, CD62L and CCR7 were found to be closely associated in Peyer’s Patch samples compared to spleen (Fig 7f).

WT and IL-13 KO mice have distinct integrins and CCR9 mRNA expression profiles in gut and splenic K^dGag_{197–205}-specific CD8⁺ T cells

Integrins $\alpha 4$, αE , $\beta 1$, $\beta 7$ and CCR9 expression were evaluated in WT BALB/c and IL-13 KO mice gut and splenic K^dGag_{197–205}-specific CD8⁺ T cells. Data revealed that all gut and splenic cells expressed integrin $\alpha 4$ mRNA and expression levels were relatively higher in spleen compared to Peyer’s patches, specifically in IL-13 KO mice where spleen vs. Peyer’s patch $p = 0.033$ (Fig 8a). In contrast, in both the groups tested, majority of hundred cell pools that expressed integrin αE were detected in Peyer’s patch (WT BALB/c ~80%, IL-13 KO ~55%) but not in spleen and expression levels were also found to be elevated in gut-K^dGag_{197–205}-specific CD8⁺ T cells (Fig 8b). Data also revealed all the cell pools expressed integrins $\beta 1$ and $\beta 7$ mRNAs and their expression levels were significantly higher in WT BALB/c and IL-13 KO splenic K^dGag_{197–205}-specific CD8⁺ T cells (in WT BALB/c and IL-13 KO groups, $\beta 1$ expression, spleen vs. Peyer’s patch $p = 0.001$; $\beta 7$ expression, spleen vs. Peyer’s patch $p = 0.01$) (Fig 8c & 8d). Furthermore, when the CCR9 and

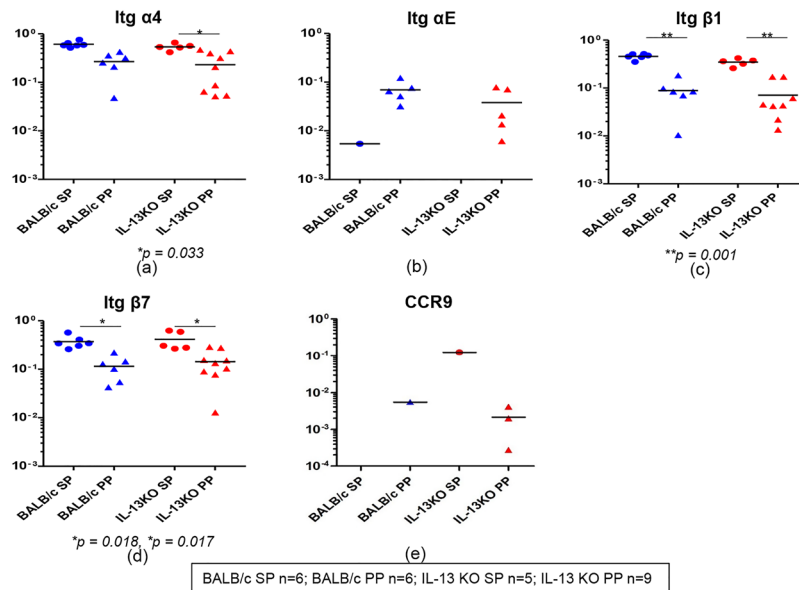


Fig 8. Evaluation of integrins $\alpha 4$, αE , $\beta 1$ and $\beta 7$ and CCR9 mRNA expression in WT BALB/c and IL-13 KO gut and splenic $K^dGag_{197-205}$ -specific $CD8^+$ T cells following i.n./i.m. vaccination. mRNA expression profiles in WT BALB/c and IL-13KO gut and splenic $K^dGag_{197-205}$ -specific $CD8^+$ T cells were evaluated using Fluidigm 48.48 dynamic arrays as described in methods. WT BALB/c spleen (SP) and Peyer's patch (PP) $n = 6$ pools of hundred $K^dGag_{197-205}$ -specific $CD8^+$ T cells are indicated by blue circle and triangle respectively. IL-13 KO mice spleen $n = 5$ and Peyer's patch $n = 9$ pools of hundred $K^dGag_{197-205}$ -specific $CD8^+$ T cells are indicated by red circles and triangles respectively. Data indicate log mRNA expression of integrin $\alpha 4$ (a) αE (b) $\beta 1$ (c) $\beta 7$ (d) and CCR9 (e) normalised to housekeeping gene L32. The experiment was repeated three times. Data represent the three experiments.

doi:10.1371/journal.pone.0126487.g008

CCR10 mRNA expression were evaluated, very low numbers of gut- $K^dGag_{197-205}$ -specific $CD8^+$ T cells (WT BALB/c, spleen 0/6 and Peyer's patch 1/6; in IL-13KO spleen 1/5 and Peyer's patch 3/9) were found to express CCR9 (Fig 8e) and no CCR10 mRNA expression was detected.

Furthermore, when the expression of integrin αL , αM , αX and αD mRNAs which are known to heterodimerize with integrin $\beta 2$ were evaluated in both the groups, no integrin αD expression was detected. Lower proportion of gut/splenic $K^dGag_{197-205}$ -specific $CD8^+$ T cells (20–30%) were found to express integrin αL and expression levels were similar in both the compartments and the two groups (Fig 9a). In contrast, higher numbers of WT BALB/c and IL-13 KO mice splenic $K^dGag_{197-205}$ -specific $CD8^+$ T cell pools were positive for integrin αM compared to Peyer's patch (WT BALB/c group, spleen 6/6 and Peyer's patch 1/6; IL-13 KO group, spleen 1/5 and Peyer's patch 4/9) and also the expression level was relatively elevated in splenic $K^dGag_{197-205}$ -specific $CD8^+$ T cells (Fig 9b). Likewise, in all the groups tested, although the proportions of cell pools positive for integrin αX were found to be similar, expression level was higher in splenic $K^dGag_{197-205}$ -specific $CD8^+$ T cells compared to Peyer's patches (Fig 9c). Interestingly, most or all cell pools expressed obtained from both mice groups expressed integrin $\beta 2$, and expression levels were relatively higher in splenic $K^dGag_{197-205}$ -specific $CD8^+$ T cells compared to Peyer's patch (Fig 9d).

IL-13 KO mice have elevated $\alpha 4\beta 7^+$ and CCR9⁺ gut $K^dGag_{197-205}$ -specific $CD8^+$ T cells

WT BALB/c and IL-13 KO mice were prime boost immunized using i.n. FPV-HIV/i.m. VV-HIV strategy. Fourteen days post booster vaccination, splenic and gut $K^dGag_{197-205}$ -specific $CD8^+$ T cell

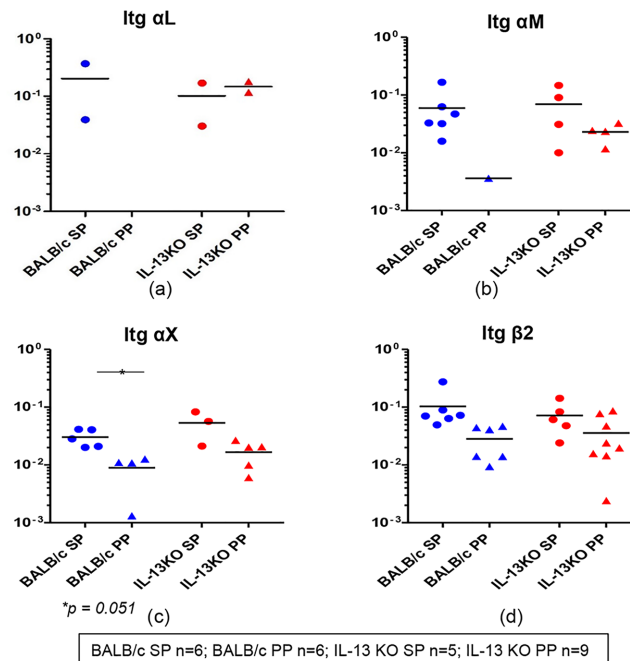


Fig 9. Evaluation of integrins α L, α M, α X and β 2 mRNA expression in WT BALB/c and IL-13 KO gut and splenic $K^dGag_{197-205}$ -specific $CD8^+$ T cells following i.n./i.m. vaccination. Exactly as in Fig 8, mRNA expression profiles in WT BALB/c and IL-13KO gut and splenic $K^dGag_{197-205}$ -specific $CD8^+$ T cells were evaluated. WT BALB/c spleen (SP) and Peyer's patch (PP) $n = 6$ pools of hundred $K^dGag_{197-205}$ -specific $CD8^+$ T cells are indicated in blue circles and triangles respectively. IL-13 KO mice spleen $n = 5$ and Peyer's patch $n = 9$ pools of hundred $K^dGag_{197-205}$ -specific $CD8^+$ T cells are indicated by red circles and triangles respectively. Data indicate log mRNA expression of integrin α L (a) α M (b) α X (c) and β 2 (d) normalised to housekeeping gene L32.

doi:10.1371/journal.pone.0126487.g009

responses were evaluated using $K^dGag_{197-205}$ -tetramer staining together with $\alpha 4\beta 7$ and CCR9 staining using FACS analysis. Data revealed that the magnitude of $K^dGag_{197-205}$ -specific splenic $CD8^+$ T cell numbers were similar between the two mice groups tested (Fig 10), which was consistent to our previous findings [12]. Notably, the percentages of $\alpha 4\beta 7^+$ splenic $K^dGag_{197-205}$ -specific $CD8^+$ T cells were much elevated in WT and IL-13 KO mice compared to CCR9 ($\alpha 4\beta 7^+ \sim 1.5\%$ and CCR9 less than 0.5%, $p < 0.0001$ (Fig 10b & 10c), but, no significant difference in expression was detected between WT BALB/c and IL-13 KO splenic groups (Fig 10b & 10c). In contrast, compared to WT mice the percentages of $\alpha 4\beta 7^+$ and CCR9 $^+$ gut- $K^dGag_{197-205}$ -specific $CD8^+$ T cells were found to be significantly elevated in IL-13 KO mice compared to the WT BALB/c (Fig 10e & 10f). When the frequency of $\alpha 4\beta 7$ and CCR9 were assessed in spleen vs. gut $K^dGag_{197-205}$ -specific $CD8^+$ T cells obtained from WT and IL-13 KO groups, threefold increase in the expression frequency of $\alpha 4\beta 7$ and CCR9 were detected in Peyer's patches ($\sim 60\%$) compared to spleen ($\sim 20\%$) (Fig 10g & 10h).

Discussion

Studies have shown that mucosal immune responses are most efficiently induced by administration of vaccines to the mucosae, whereas systemic immunization strategies rarely induce long lasting or optimal mucosal immunity and are therefore less effective against infection at the mucosal surfaces [25, 26]. The Sabin live attenuated oral polio vaccine (OPV) introduced in 1950s is a classic example of an effective mucosal vaccine. Unlike the injectable inactivated polio vaccine (IPV), OPV was shown to induce secretory IgA antibody responses at the intestinal mucosae the

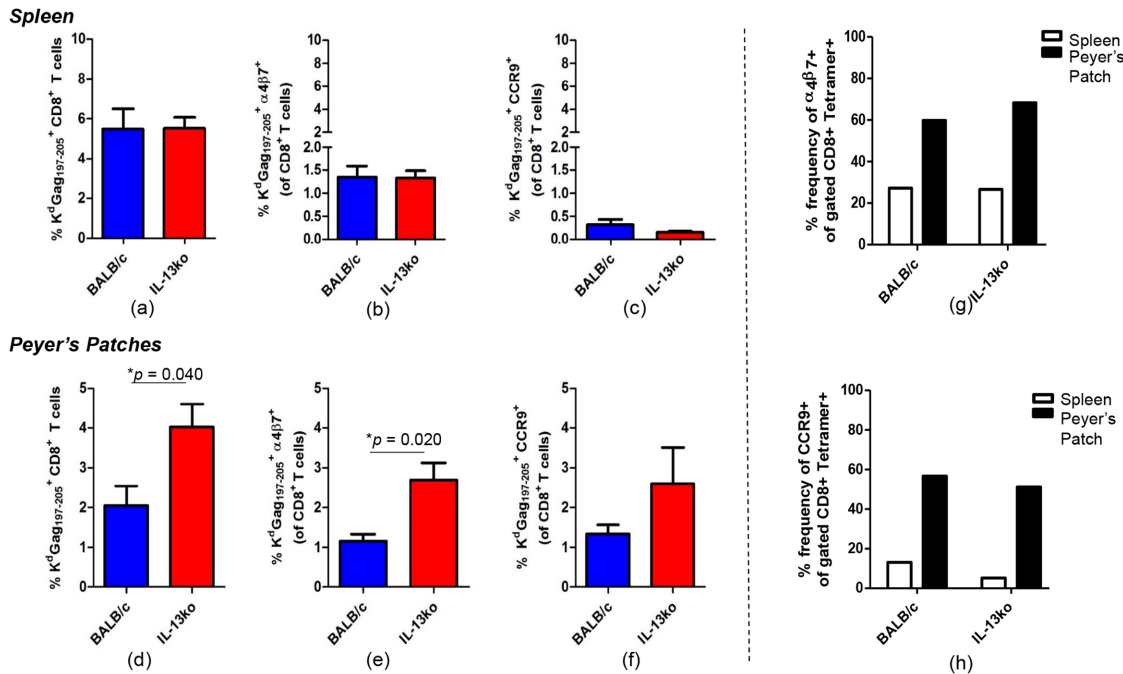


Fig 10. Evaluation of WT BALB/c and IL-13 KO gut and splenic $K^dGag_{197-205}$ -specific $CD8^+ \alpha 4\beta 7^+$ and $K^dGag_{197-205}$ -specific $CD8^+ CCR9^+$ T cells following i.n./i.m. vaccination. WT BALB/c and IL-13 KO mice were prime boost immunized using i.n. FPV-HIV/i.m. VV-HIV strategy. Fourteen days post booster vaccination, splenic and gut $K^dGag_{197-205}$ -specific $CD8^+$ T cell responses were evaluated using $K^dGag_{197-205}$ -tetramer staining together with $\alpha 4\beta 7$ and CCR9 staining using FACS analysis. The percentage of WT BALB/c (blue) and IL-13 KO (red) splenic and gut $K^dGag_{197-205}$ -tetramer $^+$ $CD8^+$ T cells (a and d), $K^dGag_{197-205}$ -tetramer $^+$ $CD8^+ \alpha 4\beta 7^+$ T cells (b and e), $K^dGag_{197-205}$ -tetramer $^+$ $CD8^+ CCR9^+$ T cells (c and f) is shown. The percentage frequency of $\alpha 4\beta 7$ and CCR9 homing marker expression on WT BALB/c and IL-13 KO splenic (g) and gut (h) $K^dGag_{197-205}$ -tetramer $^+$ $CD8^+$ T cells is also shown. Data represent 4–5 experiments.

doi:10.1371/journal.pone.0126487.g010

site of virus replication helping effective control of poliovirus, making OPV a powerful strategy for global eradication of polio [27]. We have shown that i) vaccine regime (i.e. systemic vs. mucosal delivery) can significantly influence the magnitude as well as the quality/avidity of immune response at the mucosae [9, 10] and ii), mucosal versus systemic immunization regimes can induce distinct gene expression profiles in splenic $K^dGag_{197-205}$ -specific single $CD8^+$ T cells [10]. In the current study evaluating the expression of thirty different genes in gut- $K^dGag_{197-205}$ -specific $CD8^+$ T cells using Fluidigm 48.48 dynamic arrays have further established that different vaccine delivery routes can vastly influence the gene expression profiles in mucosal and systemic compartments. Specifically, compared to purely mucosal (i.n./i.n.) FPV-HIV/VV-HIV prime-boost immunization regime, combined systemic mucosal (i.n./i.m.) and purely systemic (i.m./i.m.) immunization regimes showed enhanced expression of MIP-1 β , RANTES, and CCR5 mRNAs in gut $K^dGag_{197-205}$ -specific $CD8^+$ T cells indicating that enhanced expression of these chemokines/chemokine receptor genes were most likely driven by the systemic antigen encounter following the i.m. VV-HIV booster vaccination. Our antibody array studies have also revealed enhanced expression of RANTES by HIV-specific $CD8^+$ splenocytes following i.n. FPV-HIV/ i.m. VV-HIV immunization compared to i.m. pDNA-HIV/ i.n. FPV-HIV vaccination [6]. Furthermore, compared to WT BALB/c mice, IL-13 KO mice immunized with i.n. FPV-HIV/ i.m. VV-HIV vaccination strategy has also shown to induce higher avidity $CD8^+$ T cells with better protective efficacy [12] and this was associated with significantly enhanced RANTES mRNA expression by splenic $K^dGag_{197-205}$ -specific single memory $CD8^+$ T cells [12]. These studies also indicated that in antigen-specific $CD8^+$ T cells, RANTES is regulated by IL-4

and IL-13 [12]. The current data further substantiated these findings as absence of IL-13 correlated with higher expression of RANTES and MIP-1 β in splenic K^dGag_{197–205}-specific CD8⁺ T cells.

In previous single cell profiling studies, majority of splenic K^dGag_{197–205}-specific single (~80%) CD8⁺ T cells were found to express IFN- γ and lower proportion was found to express TNF- α (1–5%) [10]. However, in this study no IFN- γ expression was detected in the gut K^dGag_{197–205}-specific CD8⁺ T cells. In contrast, in all three immunization regimes tested, 80–90% of the gut K^dGag_{197–205}-specific CD8⁺ T cells were found to be positive for TNF- α . Interestingly, TNF- α have been associated with increased migration and proliferation of intraepithelial lymphocytes in gut [28] and this may explain the differences observed in CD8⁺ T cell cytokine specificities in spleen and gut compartments [6, 10]. Furthermore, the discrepancy in IFN- γ expression profile, compared to the previous studies [10] could also be due evaluating mRNA from 100 K^dGag_{197–205}-specific CD8⁺ T cells not single cell level using Fluidigm 48.48 dynamic array analysis which could be a major caveat. Specifically, it is likely that in a pool of hundred cells the abundance of an mRNA like IFN- γ could be extremely high and this has high potential to inhibit optimum PCR amplification of these genes [29] [Note that in this study 30 genes were amplified from a single cDNA sample obtained from 100 cells and the abundance of the 30 gene transcripts will be vastly different (for example; elevated IFN- γ vs lower levels of integrin α D mRNA). Thus, in an ideal scenario the most abundant genes will have to be diluted to obtain the optimum amplification outcomes [29]].

Surprisingly, following i.n./i.m immunization no significant differences between the control WT BALB/c and IL-13 KO gut K^dGag_{197–205}-specific CD8⁺ T cells were detected at a 100-cell level. However, previous studies in our laboratory have reported greatly elevated expression of granzyme B in IL-13 KO splenic K^dGag_{197–205}-specific single CD8⁺ T cells compared to other groups tested [12]. Similarly, when mRNA expression profiles were evaluated at a single cell level enhanced expression of RANTES, MIP-1 β , perforin and also granzymes A and B by gut K^dGag_{197–205}-specific CD8⁺ T cells were detected in IL-13 KO mice compared to WT BALB/c mice (Trivedi *et al.*, manuscript submitted). Several other recent studies also have illustrated the power and necessity of using single-cell gene expression profiling approaches in evaluating vaccine efficacy or immune outcomes following infection [30–32]. For example, recent study by Flatz *et al.*, have shown qualitative differences between CD8⁺ T cell responses following different prime-boost immunization strategies (DNA/rAd5, rAd5/rAd5 and rAd5/rLCMV) when data were analysed at a single-cell gene expression level compared to pooled analysis [31]. Current data taken together with our single-cell gene expression data (Trivedi *et al.*, manuscript submitted) clearly reveal that when evaluating the outcome of an immune response, single cell gene expression profiling has high potential to generate more powerful information than pooled cell analysis.

Current study indicated that according to the anatomical location in which the K^dGag_{197–205}-specific CD8⁺ T cells were obtained (spleen vs Peyer's patch) the mRNA expression profiles were significantly different both in WT BALB/c and IL-13 KO mice. This is consistent with studies by Masopust *et al.* [13] where they showed that anatomical location played an important role in modulating memory T cell immunity. Specifically, unlike Peyer's patches, splenic K^dGag_{197–205}-specific CD8⁺ T cells expressed CCR7 but lacked CD62L suggesting that tissue microenvironment regulated memory cell surface marker expression and memory T cell differentiation. Rapid down-regulation of CD62L by splenic K^dGag_{197–205}-specific CD8⁺ T cells has often been correlated with the loss of T cell trafficking to peripheral lymph nodes [33]. According to the current findings it appears that gut K^dGag_{197–205}-specific CD8⁺ T cells most likely retain CD62L expression which enable them to rapidly reenter lymph nodes [34, 35].

This study was one of the first to evaluate an array of integrins that are reported to be present on lymphocytes and their expression profile following different routes of vaccination and conditions. Several studies have now shown that integrins like $\alpha 4\beta 7$ is differentially expressed on T cells and they play a role in tissue-specific T cell homing in an immunization route dependent manner [22, 24, 36–38]. Interestingly, current study clearly demonstrated that in a prime-boost vaccination setting, the prime or the booster immunization could differentially influence the integrin expression profile on gut $K^dGag_{197-205}$ -specific $CD8^+$ T cells. For example; elevated numbers of integrin αE expressing $K^dGag_{197-205}$ -specific $CD8^+$ T cells were detected in gut following mucosal but not systemic priming, indicating that the mucosal micro-environment was responsible for altering the αE homing marker expression. This is consistent with another finding where integrin $\beta 7$ was also found to be up-regulated on T cells primed in mesenteric lymph nodes which home to the mucosae [37]. Integrin αE normally pairs up with $\beta 7$ and is known to facilitate retention of lymphocytes in the gut via interaction with E-cadherin [39, 40]. In this study αE and $\beta 7$ integrins were found to be more closely associated together in an i.n./i.n. vaccinated setting compared to the i.n./i.m. or i.m./i.m. vaccinated groups. Recent studies have shown that during mucosal T cell priming, dendritic cells play a critical role in imprinting antigen-specific T cells with different homing markers and this is also retinoic acid dependent [20, 41]. Moreover, integrins $\alpha 4$ and $\beta 7$ were found to be more closely associated together in all vaccinated groups tested compared to integrins $\alpha 4$ and $\beta 1$. It is now well established that integrin heterodimer $\alpha 4\beta 7$ help T cell migration to the gut mucosae [20, 22]. In the current study, following i.m. booster vaccination significantly enhanced integrin $\alpha 4$ mRNA expressing gut $K^dGag_{197-205}$ -specific effector $CD8^+$ T cells were detected. This suggested that i.m. booster vaccination may have high potential to promote the expansion of mucosally originated antigen-specific $CD8^+$ T cells (primed at the mucosae) in the systemic compartment. This hypothesis can be further substantiate as, higher $\alpha 4$ and $\beta 7$ mRNA were detected also in splenic $K^dGag_{197-205}$ -specific $CD8^+$ T cells suggesting that these cells may continue to circulate between the mucosal and systemic compartments. However, the full dynamics involved in tissue environment and the role of integrins in T cell homing is yet to be discovered.

Furthermore, following mucosal and systemic immunization all gut- $K^dGag_{197-205}$ -specific $CD8^+$ T cells were found to express integrin $\beta 2$. Studies have shown that integrin $\beta 2$ (known to heterodimerize with αL , αM , αX and αD) play a critical role in T cell activation and in trans-endothelial migration [42, 43]. Unlike αL , αM , and αX , integrin $\beta 2$ were found to be closely associated with integrin αD in an i.n./i.n. setting compared to the other two strategies tested. However, the function of integrin αD in a vaccination context has not yet been fully characterized. In contrast, the integrins αM and $\beta 2$ were found to be relatively higher and closely associated in an i.n./i.m. and i.m./i.m. setting, further highlighting that immunization route/strategy can significantly regulate the expression of integrins on T cells.

Interestingly, compared to WT control the number of gut $K^dGag_{197-205}$ -specific $CD8^+$ T cells expressing gut-homing markers $\alpha 4\beta 7$ and CCR9 protein were found to be significantly higher in IL-13 KO as well as IL-4 KO mice (unpublished observation in our laboratory). New vaccines that transiently inhibited IL-4/IL-13 [44, 45] also enhanced integrin $\alpha 4$ mRNA expression in gut $K^dGag_{197-205}$ -specific single $CD8^+$ T cells (Trivedi *et al.*, manuscript submitted). These observations suggest that inhibition of IL-13 or IL-4, most likely help increase trafficking of $K^dGag_{197-205}$ -specific $CD8^+$ T cells to gut mucosae. Other studies also have shown the role of cytokines such as IL-12, IL-4 and TGF- β in regulating tissue-specific lymphocyte trafficking [46–48]. We have established that transient inhibition of IL-4 and IL-13 can significantly modulate the antigen presenting cell subsets at the vaccination site and induce a high avidity T cell repertoire [49]. Thus, we suggest that IL-4/IL-13 depleted cell milieu most likely help create a unique T cell subset with specific homing capacities to the

mucosal sites. The exact mechanisms how IL-4 and/or IL-13 modulate T cell homing warrants further investigation.

Collectively, the current data indicated that out of the thirty genes tested, at the pooled 100 cell level, the MIP-1 β , RANTES, CCR5, perforin and integrin α 4 mRNA expression were significantly different in the three immunization regimes tested. Similarly, the expression levels of MIP-1 α , MIP-1 β , RANTES, integrins α 4, β 1 and β 7 mRNAs were markedly different between mucosal and systemic compartments. These observations further emphasize that the route of vaccine delivery, tissue microenvironment plus the cytokine milieu (specifically IL-13) can significantly influence the gene expression profiles of K^dGag_{197–205}-specific CD8⁺ T cells and modulate their functional specificities (high versus low avidity) as well as cell homing capabilities. In conclusion, the above findings corroborate that these factors have to be seriously taken into consideration when designing novel/effective vaccines strategies that can induce optimal mucosal CD8⁺ T cell immunity against chronic pathogens such as HIV-1.

Materials and Methods

Immunization of mice

Pathogen-free 6 to 8 week old female WT BALB/c and IL-13 KO mice on BALB/c background were purchased from the Australian Phenomics Facility, the Australian National University (ANU). WT BALB/c mice were prime-boost immunized with 1×10^7 PFU rFPV followed by 1×10^7 PFU rVV expressing HIV-antigens, under isoflurane anesthesia 2 weeks apart using mucosal and systemic routes of vaccination. IL-13 KO mice were prime-boost immunized with i.n. rFPV/ i.m. rVV. The i.n. rFPV was given in a final volume of 20–25 μ l, where i.m. rVV immunization was delivered in a 100 μ l volume. All viruses were diluted in sterile phosphate-buffered saline (PBS) and then sonicated, to obtain homogeneous viral suspensions before delivery.

Ethics Statement

All animals were maintained and experiments were performed in accordance with the Australian NHMRC guidelines within the Australian Code of Practice for the Care and Use of Animals for Scientific Purposes and in accordance with guidelines approved by the Australian National University Animal Experimentation and Ethics Committee (AEEC). This study was approved by the AEEC and listed under ANU ethics protocol number A2011/018. All animals were anesthetized using isoflurane and monitored daily. At the end of the experiments were ethically sacrificed using cervical dislocation in accordance with the above AEEC approved protocols.

Mucosal and systemic lymphocytes preparation

The mice were euthanized using cervical dislocation, spleen and Peyer's patches were removed and single cell suspensions were prepared as described previously [45, 50]. Briefly, the spleen cells were passed through a cell strainer and were treated with red blood cell lysis buffer for 7 min at room temperature, cells were then washed, and suspended in complete RPMI (RPMI supplemented with 7% fetal calf serum, 20 mM 4-(2-hydroxyethyl)-1-piperazineethanesulfonic acid, 30 μ g ml⁻¹ penicillin, 50 μ g ml⁻¹ streptomycin, 2 mM sodium pyruvate (Gibco-Invitrogen, Auckland, NZ), and 50 M 2-mercaptoethanol (Sigma, St Louis, MO), and kept at 4°C until use, similarly Peyer's patches were prepared without the red cell lysis step. The Peyer's patch cells were filtered through the small piece of gauze to remove debris prior to final suspension in complete RPMI medium.

Tetramer and homing marker staining

Allophycocyanin (APC) conjugated K^dGag_{197–205} tetramers were synthesized at the Bio-Molecular Resource Facility at The John Curtin School of Medical Research (BRF/JCSMR), ANU. Tetramer staining was performed as described previously [9, 10]. Briefly, 2 X 10⁶ splenocytes and Peyer's patches were stained with anti-CD8 α FITC antibody and APC conjugated K^dGag_{197–205} tetramer at room temperature for 40 min. After washing cells twice with FACS buffer (PBS with 1% fetal calf serum), the cell pellets were resuspended in 0.5% PFA (except for studies involving cell sorting). For gene expression profile analysis, K^dGag_{197–205}-specific hundred cells (from pooled splenocytes or Peyer's patches) were sorted into 96-well plates using stringent gating strategy as described previously [10] [40]. NOTE: The purpose of this study was to assess the expression of these genes specifically in tetramer-specific CD8 T cells (with no prior antigen stimulation) similar to our previous studies. It is well established that antigen-activation (stimulation with specific-peptide) and tetramer staining cannot be performed concurrently, as i) stimulation prior to tetramer binding can lead to loss of tetramer staining due to down-regulation of the T-cell receptors and ii) peptide and tetramer competes for the same binding site and this leads to a competition and reduce tetramer staining.

For homing markers analysis, first the cells were stained with APC-conjugated tetramer for 40 min and then were surface stained with biotin labelled anti-mouse LPAM-1 or α 4 β 7 and FITC conjugated anti-mouse CCR9 antibodies for 25 min at 4°C, followed by brilliant violet 421 streptavidin (useful for indirect staining of biotin labelled α 4 β 7 primary antibody) for another 25 min at 4°C. Cells were fixed and total 10⁶ events per sample were collected using Fortessa flow cytometer (Becton-Dickinson), and the results were analyzed using Cell Quest Pro software. Note: frequency of homing marker expression out of the total K^dGag_{197–205}-tetramer⁺ CD8⁺ T cell population was calculated as in Xi *et. al.* [50].

Evaluation of mRNA expression in hundred K^dGag_{197–205}-tetramer⁺ CD8⁺ T cells

K^dGag_{197–205} tetramer⁺ CD8⁺ hundred cells from spleen and/ Peyer's patches were sorted using cell FACS Aria I (BD Biosciences) into 96-well plates containing CellsDirect qRT-PCR reaction buffer (Invitrogen), Platinum Taq polymerase / SuperScript III reverse transcriptase (Invitrogen), a mixture of Taqman primer-probes at 0.2X concentration specific for the transcripts of interest, as listed in Table 1 (Applied Biosystems), and SuperaseIn RNase inhibitor. Immediately following cell sorting, samples were centrifuged, and subjected to 20 cycles of pre amplification using polymerase chain reaction (PCR) (cell cycling as: 1 X 50°C 15 min for the reverse transcription then 1 X 95°C 2 min for reverse transcriptase inactivation and Taq polymerase activation, followed by 20 X 95°C 15 s and 60°C 4 min amplification cycle). Subsequently, the pre-amplified cDNA was stored at -20°C until analysis and was diluted with dH₂O (1:2) prior to qPCR reaction. Each pre-amplified cDNA sample was then separated into 48 separate reactions for qPCR analysis using the BioMark 48.48 dynamic array nanofluidic chip (Fluidigm Inc., USA) according to manufacturer's instruction.

Briefly, following hydraulic chip priming, 47 preamplified cDNA samples plus one no template standard were mixed with a mild detergent loading solution to allow capillary flow, and the samples were added to the sample inlets of 48.48 nanofluidic chip (Fluidigm, Inc.), 30 individual Taqman primer-probe mixtures (Applied Biosystems) specific for individual transcripts of interest listed in Table 1 along with assay loading solution were also added into the specific assay inlets of the 48.48 nanofluidic chip, allowing a combination of each sample to mix with each primer-probe assay in every possible combination (a total of 2304 reactions). The chip was then thermo-cycled through 40 cycles and Taqman primer-probe fluorescence in the FAM

channel was detected using the CCD (charge-coupled device) camera attached to the BioMark HD system, normalized by ROX (6-carboxy-X-rhodamine) intensity. The statistical analyses of the data were performed as described below.

Statistical analysis

Amplification signals were analysed and Ct values were determined using Fluidigm's real-time PCR analysis software version 4. The Ct values of genes were normalized against housekeeping gene ribosomal protein L32 ($\Delta Ct = Ct_{\text{gene}} - Ct_{L32}$), data represents the mRNA fold expression relative to housekeeping gene ($2^{-\Delta Ct}$). The error bars represents standard error of mean and the *p* values were determined using one-way analysis of variance followed by Sidak multiple comparison test or Dunnett (2-sided) post tests using IBM SPSS version 21. For the flow-cytometer analysis, the standard error of the mean and *p* values were determined using two-tailed Student's *t*-test, using GraphPad Prism software version 5. Raw Fluidigm's real-time PCR data can be found in supporting information ([S1](#) and [S2](#) Datasets).

Supporting Information

S1 Dataset. Ct values of genes expressed in gut HIV-specific CD8 T cells following different routes of immunization.

(XLSX)

S2 Dataset. Ct values of genes expressed in systemic and mucosal HIV-specific CD8 T cells obtained from WT and IL-13 KO mice.

(XLSX)

Acknowledgments

The authors would like to thank Dr. David Boyle for providing the parent vaccine constructs. Dr. Kerong Zhang and Dr. Peter Milburn at the ACRF BRF/JCSMR ANU for synthesising the HIV-specific tetramers and help with BioMark 48.48 dynamic array analysis respectively. Michael Devoy at the MCRF/JCSMR ANU for his technical assistance with flow cytometry and cell sorting. Annette Buchanan and Jayshree Ravichandran for their help in the laboratory.

Author Contributions

Conceived and designed the experiments: ST CR. Performed the experiments: ST. Analyzed the data: ST. Contributed reagents/materials/analysis tools: CR. Wrote the paper: ST CR.

References

1. Belyakov IM, Ahlers JD, Nabel GJ, Moss B, Berzofsky JA. Generation of functionally active HIV-1 specific CD8+ CTL in intestinal mucosa following mucosal, systemic or mixed prime-boost immunization. *Virology*. 2008; 381(1):106–15. Epub 2008/09/17. doi: [10.1016/j.virol.2008.08.019](https://doi.org/10.1016/j.virol.2008.08.019) PMID: [18793787](https://pubmed.ncbi.nlm.nih.gov/18793787/).
2. Belyakov IM, Derby MA, Ahlers JD, Kelsall BL, Earl P, Moss B, et al. Mucosal immunization with HIV-1 peptide vaccine induces mucosal and systemic cytotoxic T lymphocytes and protective immunity in mice against intrarectal recombinant HIV-vaccinia challenge. *P Natl Acad Sci USA*. 1998; 95(4):1709–14. doi: [10.1073/pnas.95.4.1709](https://doi.org/10.1073/pnas.95.4.1709). WOS:000072115900064. PMID: [9465081](https://pubmed.ncbi.nlm.nih.gov/9465081/)
3. Eo SK, Gierynska M, Kamar AA, Rouse BT. Prime-boost immunization with DNA vaccine: mucosal route of administration changes the rules. *Journal of immunology*. 2001; 166(9):5473–9. PMID: [11313385](https://pubmed.ncbi.nlm.nih.gov/11313385/).
4. Kozlowski PA, Cu-Uvin S, Neutra MR, Flanigan TP. Comparison of the oral, rectal, and vaginal immunization routes for induction of antibodies in rectal and genital tract secretions of women. *Infection and immunity*. 1997; 65(4):1387–94. Epub 1997/04/01. PMID: [9119478](https://pubmed.ncbi.nlm.nih.gov/9119478/); PubMed Central PMCID: [PMCPmc175144](https://pubmed.ncbi.nlm.nih.gov/PMCPmc175144/).
5. Kent SJ, Dale CJ, Ranasinghe C, Stratov I, De Rose R, Chea S, et al. Mucosally-administered human-simian immunodeficiency virus DNA and fowlpoxvirus-based recombinant vaccines reduce acute phase

- viral replication in macaques following vaginal challenge with CCR5-tropic SHIVSF162P3. *Vaccine*. 2005; 23(42):5009–21. doi: [10.1016/j.vaccine.2005.05.032](https://doi.org/10.1016/j.vaccine.2005.05.032). ISI:000232265200006. PMID: [15985317](https://pubmed.ncbi.nlm.nih.gov/15985317/)
6. Ranasinghe C, Eyers F, Stambas J, Boyle DB, Ramshaw IA, Ramsay AJ. A comparative analysis of HIV-specific mucosal/systemic T cell immunity and avidity following rDNA/rFPV and poxvirus—poxvirus prime boost immunisations. *Vaccine*. 2011; 29(16):3008–20. doi: [10.1016/j.vaccine.2011.01.106](https://doi.org/10.1016/j.vaccine.2011.01.106) PMID: [21352941](https://pubmed.ncbi.nlm.nih.gov/21352941/)
 7. Almeida JR, Price DA, Papagno L, Arkoub ZA, Sauce D, Bornstein E, et al. Superior control of HIV-1 replication by CD8+ T cells is reflected by their avidity, polyfunctionality, and clonal turnover. *J Exp Med*. 2007; 204(10):2473–85. Epub 2007/09/26. doi: [jem.20070784](https://doi.org/10.1084/jem.20070784) [pii] doi: [10.1084/jem.20070784](https://doi.org/10.1084/jem.20070784) PMID: [17893201](https://pubmed.ncbi.nlm.nih.gov/17893201/); PubMed Central PMCID: PMC2118466.
 8. Betts MR, Nason MC, West SM, De Rosa SC, Migueles SA, Abraham J, et al. HIV nonprogressors preferentially maintain highly functional HIV-specific CD8+ T cells. *Blood*. 2006; 107(12):4781–9. Epub 2006/02/10. doi: [2005-12-4818](https://doi.org/10.1182/blood-2005-12-4818) [pii] doi: [10.1182/blood-2005-12-4818](https://doi.org/10.1182/blood-2005-12-4818) PMID: [16467198](https://pubmed.ncbi.nlm.nih.gov/16467198/); PubMed Central PMCID: PMC1895811.
 9. Ranasinghe C, Medveczky JC, Woltring D, Gao K, Thomson S, Coupar BE, et al. Evaluation of fowl-pox-vaccinia virus prime-boost vaccine strategies for high-level mucosal and systemic immunity against HIV-1. *Vaccine*. 2006; 24(31–32):5881–95. Epub 2006/06/09. doi: [S0264-410X\(06\)00456-7](https://doi.org/10.1016/j.vaccine.2006.04.023) [pii]. doi: [10.1016/j.vaccine.2006.04.023](https://doi.org/10.1016/j.vaccine.2006.04.023) PMID: [16759767](https://pubmed.ncbi.nlm.nih.gov/16759767/).
 10. Ranasinghe C, Turner SJ, McArthur C, Sutherland DB, Kim JH, Doherty PC, et al. Mucosal HIV-1 pox virus prime-boost immunization induces high-avidity CD8+ T cells with regime-dependent cytokine/granzyme B profiles. *Journal of immunology*. 2007; 178(4):2370–9. Epub 2007/02/06. doi: [178/4/2370](https://doi.org/10.1093/infdis/jni143) [pii]. PMID: [17277143](https://pubmed.ncbi.nlm.nih.gov/17277143/).
 11. Wijesundara DK, Ranasinghe C, Jackson RJ, Lidbury BA, Parish CR, Quah BJC. Use of an *In Vivo* FTA Assay to Assess the Magnitude, Functional Avidity and Epitope Variant Cross-Reactivity of T Cell Responses Following HIV-1 Recombinant Poxvirus Vaccination. *PLoS ONE*. 2014; 9(8):e105366. doi: [10.1371/journal.pone.0105366](https://doi.org/10.1371/journal.pone.0105366) PMID: [25170620](https://pubmed.ncbi.nlm.nih.gov/25170620/)
 12. Ranasinghe C, Ramshaw IA. Immunisation route-dependent expression of IL-4/IL-13 can modulate HIV-specific CD8(+) CTL avidity. *Eur J Immunol*. 2009; 39(7):1819–30. Epub 2009/07/08. doi: [10.1002/eji.200838995](https://doi.org/10.1002/eji.200838995) PMID: [19582753](https://pubmed.ncbi.nlm.nih.gov/19582753/).
 13. Masopust D, Vezys V, Wherry EJ, Barber DL, Ahmed R. Cutting edge: gut microenvironment promotes differentiation of a unique memory CD8 T cell population. *Journal of immunology*. 2006; 176(4):2079–83. Epub 2006/02/04. PMID: [16455963](https://pubmed.ncbi.nlm.nih.gov/16455963/).
 14. Takenaka S, McCormick S, Safroneeva E, Xing Z, Gauldie J. Influence of the tissue microenvironment on Toll-like receptor expression by CD11c+ antigen-presenting cells isolated from mucosal tissues. *Clinical and Vaccine Immunology*. 2009; 16(11):1615–23. doi: [10.1128/CVI.00216-09](https://doi.org/10.1128/CVI.00216-09) PMID: [19776199](https://pubmed.ncbi.nlm.nih.gov/19776199/)
 15. Baaten BJ, Cooper AM, Swain SL, Bradley LM. Location, location, location: the impact of migratory heterogeneity on T cell function. *Frontiers in Immunology*. 2013; 4. doi: [10.3389/fimmu.2013.00311](https://doi.org/10.3389/fimmu.2013.00311)
 16. Hathaway LJ, Kraehenbuhl JP. The role of M cells in mucosal immunity. *Cellular and molecular life sciences: CMLS*. 2000; 57(2):323–32. Epub 2000/04/15. PMID: [10766026](https://pubmed.ncbi.nlm.nih.gov/10766026/).
 17. Neutra MR, Frey A, Kraehenbuhl JP. Epithelial M cells: gateways for mucosal infection and immunization. *Cell*. 1996; 86(3):345–8. Epub 1996/08/09. doi: [S0092-8674\(00\)80106-3](https://doi.org/10.1016/S0092-8674(00)80106-3) [pii]. PMID: [8756716](https://pubmed.ncbi.nlm.nih.gov/8756716/).
 18. Mora JR, Bono MR, Manjunath N, Weninger W, Cavanagh LL, Roseblatt M, et al. Selective imprinting of gut-homing T cells by Peyer's patch dendritic cells. *Nature*. 2003; 424(6944):88–93. Epub 2003/07/04. doi: [10.1038/nature01726](https://doi.org/10.1038/nature01726) PMID: [12840763](https://pubmed.ncbi.nlm.nih.gov/12840763/).
 19. Stagg AJ, Kamm MA, Knight SC. Intestinal dendritic cells increase T cell expression of alpha4beta7 integrin. *Eur J Immunol*. 2002; 32(5):1445–54. Epub 2002/05/01. doi: [10.1002/1521-4141\(200205\)32:5<1445::AID-IMMU1445>3.0.CO;2-E](https://doi.org/10.1002/1521-4141(200205)32:5<1445::AID-IMMU1445>3.0.CO;2-E) PMID: [11981833](https://pubmed.ncbi.nlm.nih.gov/11981833/).
 20. Iwata M, Hirakiyama A, Eshima Y, Kagechika H, Kato C, Song SY. Retinoic acid imprints gut-homing specificity on T cells. *Immunity*. 2004; 21(4):527–38. Epub 2004/10/16. doi: [10.1016/j.immuni.2004.08.011](https://doi.org/10.1016/j.immuni.2004.08.011) PMID: [15485630](https://pubmed.ncbi.nlm.nih.gov/15485630/).
 21. Jespers V, Harandi AM, Hinkula J, Medagliani D, Le Grand R, Stahl-Hennig C, et al. Assessment of mucosal immunity to HIV-1. Expert review of vaccines. 2010; 9(4):381–94. doi: [10.1586/erv.10.21](https://doi.org/10.1586/erv.10.21) PMID: [20370549](https://pubmed.ncbi.nlm.nih.gov/20370549/).
 22. Kantele A, Zivny J, Hakkinen M, Elson CO, Mestecky J. Differential homing commitments of antigen-specific T cells after oral or parenteral immunization in humans. *Journal of immunology*. 1999; 162(9):5173–7. Epub 1999/05/05. PMID: [10227989](https://pubmed.ncbi.nlm.nih.gov/10227989/).
 23. Cerwenka A, Morgan TM, Harmsen AG, Dutton RW. Migration kinetics and final destination of type 1 and type 2 CD8 effector cells predict protection against pulmonary virus infection. *J Exp Med*. 1999; 189(2):423–34. Epub 1999/01/20. PMID: [9892624](https://pubmed.ncbi.nlm.nih.gov/9892624/); PubMed Central PMCID: PMC2192982.

24. Rose JR, Williams MB, Rott LS, Butcher EC, Greenberg HB. Expression of the mucosal homing receptor alpha4beta7 correlates with the ability of CD8+ memory T cells to clear rotavirus infection. *J Virol*. 1998; 72(1):726–30. Epub 1998/01/07. PMID: [9420279](#); PubMed Central PMCID: PMC109428.
25. Neutra MR, Kozlowski PA. Mucosal vaccines: the promise and the challenge. *Nature reviews Immunology*. 2006; 6(2):148–58. Epub 2006/02/24. doi: [10.1038/nri1777](#) PMID: [16491139](#).
26. Ogra PL, Faden H, Welliver RC. Vaccination strategies for mucosal immune responses. *Clinical microbiology reviews*. 2001; 14(2):430–45. Epub 2001/04/09. doi: [10.1128/cmr.14.2.430-445.2001](#) PMID: [11292646](#); PubMed Central PMCID: PMCPmc88982.
27. Holmgren J, Czerkinsky C. Mucosal immunity and vaccines. *Nature medicine*. 2005; 11(4 Suppl): S45–53. Epub 2005/04/07. doi: [10.1038/nm1213](#) PMID: [15812489](#).
28. Ebert EC. Tumour necrosis factor-alpha enhances intraepithelial lymphocyte proliferation and migration. *Gut*. 1998; 42(5):650–5. Epub 1998/07/11. PMID: [9659158](#); PubMed Central PMCID: PMCPmc1727124.
29. Nolan T, Hands RE, Bustin SA. Quantification of mRNA using real-time RT-PCR. *Nat Protocols*. 2006; 1(3):1559–82. PMID: [17406449](#)
30. Arsenio J, Kakaradov B, Metz PJ, Kim SH, Yeo GW, Chang JT. Early specification of CD8+ T lymphocyte fates during adaptive immunity revealed by single-cell gene-expression analyses. *Nature immunology*. 2014; 15(4):365–72. Epub 2014/03/04. doi: [10.1038/ni.2842](#) PMID: [24584088](#); PubMed Central PMCID: PMCPmc3968536.
31. Flatz L, Roychoudhuri R, Honda M, Filali-Mouhim A, Goulet JP, Kettaf N, et al. Single-cell gene-expression profiling reveals qualitatively distinct CD8 T cells elicited by different gene-based vaccines. *Proc Natl Acad Sci U S A*. 2011; 108(14):5724–9. Epub 2011/03/23. doi: [10.1073/pnas.1013084108](#) PMID: [21422297](#); PubMed Central PMCID: PMCPmc3078363.
32. Chattopadhyay PK, Gierahn TM, Roederer M, Love JC. Single-cell technologies for monitoring immune systems. *Nature immunology*. 2014; 15(2):128–35. doi: [10.1038/ni.2796](#) PMID: [24448570](#)
33. Hamann A, Klugewitz K, Austrup F, Jablonski-Westrich D. Activation induces rapid and profound alterations in the trafficking of T cells. *Eur J Immunol*. 2000; 30(11):3207–18. Epub 2000/11/28. doi: [10.1002/1521-4141\(200011\)30:11<#60:3207::aid-immu3207>3.0.co:2-I](#) PMID: [11093136](#).
34. Galkina E, Tanousis K, Preece G, Tolaini M, Kioussis D, Florey O, et al. L-selectin shedding does not regulate constitutive T cell trafficking but controls the migration pathways of antigen-activated T lymphocytes. *J Exp Med*. 2003; 198(9):1323–35. Epub 2003/11/05. doi: [10.1084/jem.20030485](#) PMID: [14597735](#); PubMed Central PMCID: PMCPmc2194256.
35. Venturi GM, Tu L, Kadono T, Khan AI, Fujimoto Y, Oshel P, et al. Leukocyte Migration Is Regulated by L-Selectin Endoproteolytic Release. *Immunity*. 2003; 19(5):713–24. doi: [10.1016/S1074-7613\(03\)00295-4](#) PMID: [14614858](#)
36. Sheasley-O'Neill SL, Brinkman CC, Ferguson AR, Dispenza MC, Engelhard VH. Dendritic cell immunization route determines integrin expression and lymphoid and nonlymphoid tissue distribution of CD8 T cells. *Journal of immunology*. 2007; 178(3):1512–22. Epub 2007/01/24. PMID: [17237400](#).
37. Campbell DJ, Butcher EC. Rapid acquisition of tissue-specific homing phenotypes by CD4(+) T cells activated in cutaneous or mucosal lymphoid tissues. *J Exp Med*. 2002; 195(1):135–41. Epub 2002/01/10. PMID: [11781372](#); PubMed Central PMCID: PMCPmc2196018.
38. Dudda JC, Simon JC, Martin S. Dendritic cell immunization route determines CD8+ T cell trafficking to inflamed skin: role for tissue microenvironment and dendritic cells in establishment of T cell-homing subsets. *Journal of immunology*. 2004; 172(2):857–63. Epub 2004/01/07. PMID: [14707056](#).
39. Agace WW, Higgins JM, Sadasivan B, Brenner MB, Parker CM. T-lymphocyte-epithelial-cell interactions: integrin alpha(E)(CD103)beta(7), LEEP-CAM and chemokines. *Current opinion in cell biology*. 2000; 12(5):563–8. Epub 2000/09/09. PMID: [10978890](#).
40. Schon MP, Arya A, Murphy EA, Adams CM, Strauch UG, Agace WW, et al. Mucosal T lymphocyte numbers are selectively reduced in integrin alpha E (CD103)-deficient mice. *Journal of immunology*. 1999; 162(11):6641–9. Epub 1999/06/03. PMID: [10352281](#).
41. Sigmundsdottir H, Butcher EC. Environmental cues, dendritic cells and the programming of tissue-selective lymphocyte trafficking. *Nature immunology*. 2008; 9(9):981–7. Epub 2008/08/20. doi: [10.1038/ni.f.208](#) PMID: [18711435](#); PubMed Central PMCID: PMCPmc3171274.
42. Hynes RO. Integrins: versatility, modulation, and signaling in cell adhesion. *Cell*. 1992; 69(1):11–25. PMID: [1555235](#).
43. Huleatt JW, Lefrançois L. β 2 Integrins and ICAM-1 Are Involved in Establishment of the Intestinal Mucosal T Cell Compartment. *Immunity*. 1996; 5(3):263–73. doi: [10.1016/S1074-7613\(00\)80321-0](#) PMID: [8808681](#)
44. Jackson RJ, Worley M, Trivedi S, Ranasinghe C. Novel HIV IL-4R antagonist vaccine strategy can induce both high avidity CD8 T and B cell immunity with greater protective efficacy. *Vaccine*. 2014; 20(14):01136–0. Epub 2014/08/26. doi: [10.1016/j.vaccine.2014.08.023](#) PMID: [25151041](#).

45. Ranasinghe C, Trivedi S, Stambas J, Jackson RJ. Unique IL-13/Ralpha2-based HIV-1 vaccine strategy to enhance mucosal immunity, CD8(+) T-cell avidity and protective immunity. *Mucosal immunology*. 2013; 6(6):1068–80. Epub 2013/02/14 06:00. doi: [10.1038/mi.2013.1](https://doi.org/10.1038/mi.2013.1) PMID: [23403475](https://pubmed.ncbi.nlm.nih.gov/23403475/).
46. Chin YH, Cai JP, Xu XM. Tissue-specific homing receptor mediates lymphocyte adhesion to cytokine-stimulated lymph node high endothelial venule cells. *Immunology*. 1991; 74(3):478–83. Epub 1991/11/01. PMID: [1769695](https://pubmed.ncbi.nlm.nih.gov/1769695/); PubMed Central PMCID: [PMCPmc1384643](https://pubmed.ncbi.nlm.nih.gov/pmc/articles/PMC1384643/).
47. Wagers AJ, Waters CM, Stoolman LM, Kansas GS. Interleukin 12 and interleukin 4 control T cell adhesion to endothelial selectins through opposite effects on alpha 1, 3-fucosyltransferase VII gene expression. *J Exp Med*. 1998; 188(12):2225–31. Epub 1998/12/22. PMID: [9858509](https://pubmed.ncbi.nlm.nih.gov/9858509/); PubMed Central PMCID: [PMCPmc2212430](https://pubmed.ncbi.nlm.nih.gov/pmc/articles/PMC2212430/).
48. Lim SP, Leung E, Krissansen GW. The beta7 integrin gene (Itgb-7) promoter is responsive to TGF-beta1: defining control regions. *Immunogenetics*. 1998; 48(3):184–95. Epub 1998/07/31. PMID: [9683663](https://pubmed.ncbi.nlm.nih.gov/9683663/).
49. Trivedi S, Jackson RJ, Ranasinghe C. Different HIV pox viral vector-based vaccines and adjuvants can induce unique antigen presenting cells that modulate CD8 T cell avidity. *Virology*. 2014; 468–470(0):479–89. doi: [10.1016/j.virol.2014.09.004](https://doi.org/10.1016/j.virol.2014.09.004)
50. Xi Y, Day SL, Jackson RJ, Ranasinghe C. Role of novel type I interferon epsilon in viral infection and mucosal immunity. *Mucosal immunology*. 2012; 5(6):610–22. Epub 2012/05/24. doi: [10.1038/mi.2012.35](https://doi.org/10.1038/mi.2012.35) PMID: [22617838](https://pubmed.ncbi.nlm.nih.gov/22617838/)